American Mineralogist, Volume 73, pages 140–144, 1988

Optical spectrum, site occupancy, and oxidation state of Mn in montmorillonite

David M. Sherman, Norma Vergo
U.S. Geological Survey, 959 National Center, Reston, Virginia 22092, U.S.A.

Abstract

Optical (diffuse-reflectance) spectra are used to characterize the crystal chemistry of Mn in pegmatite-associated montmorillonite. The optical spectra indicate that Mn is in the 3+ oxidation state and show Mn^{3+} ligand-field transitions near 10 400, 18 800, 20 600, and 22 400 cm^{-1}. As indicated from the number and energies of the ligand-field absorption bands, the Mn^{3+} coordination site has undergone a tetragonal distortion associated with the Jahn-Teller effect. Further distortion has eliminated even the tetragonal symmetry. Assuming that the Mn site is approximately tetragonal, however, the ligand-field theory parameters $10Dq$, Ds, and Dt are estimated to be 18 800, 1934, and 533 cm^{-1}. The large Jahn-Teller distortion of the Mn^{3+} coordination site may explain the limited solubility of Mn^{3+} cations in montmorillonite and the absence of a manganian (Mn^{3+}) smectite end-member phase.

Introduction

Montmorillonites found as pocket clay in granitic pegmatites often have relatively high Mn contents (>0.1% as MnO). Such pegmatite clays have a characteristic rose-pink color that has been attributed to the presence of Mn (e.g., Foord et al., 1986). It is generally assumed that Mn in smectites is in the Mn^{2+} oxidation state (e.g., Weaver and Pollard, 1973). However, higher oxidation states of Mn are often found in other pegmatite minerals (e.g., Mn^{3+}, Mn^{4+} in tourmaline) and the possibility of Mn^{3+} or Mn^{4+} cations in montmorillonite should be considered. Knowing the redox state of Mn in pegmatite clay minerals may help constrain the oxygen fugacity during cooling and subsequent alteration of primary pegmatite minerals.

Optical spectra provide a useful means of characterizing the crystal chemistry of transition-metal cations in minerals. For clay minerals, which do not form crystals large enough for measuring polarized single-crystal absorption spectra, the most useful technique is diffuse-reflectance spectroscopy. In this paper, visible to near-infrared diffuse-reflectance spectra are use to characterize the crystal chemistry of Mn in pegmatite clay.

Experimental details

Materials and methods

Two of the samples analyzed in this study are from the Smithsonian Institution (National Museum of Natural History) collection. NMNH 101836 is from Veracruz, Mexico, and NMNH R7452 is from Greenwood, Maine. These samples were originally described by Ross and Hendricks (1945). A third sample (K-P) is from the Katrina mine (Pala district), San Diego County, California, and was described by Foord et al. (1986). In each of these localities, the montmorillonite occupies fractures and pockets in pegmatite bodies.

Detailed characterization of the samples was done to confirm that the Mn was not associated with some minor accessory phase. Samples were dispersed in distilled water using an ultrasonic probe and size separated by centrifugation to yield the <2-μm size fraction. Diffractometer scans of random-orientation mounts of the <2-μm size fraction were done using Ni-filtered Cu radiation. This size fraction, which contained only smectite, was then oriented by centrifugation on a ceramic tile, following the methods of Kinter and Diamond (1956). X-ray diffraction patterns were run on untreated, glycol-saturated, K-saturated, Mg-saturated, and heat-treated (300 °C for 2 h and 550 °C for 2 h samples. Samples were saturated with Mg and K using the procedures outlined in Jackson (1956). Glycol solvation was achieved by direct application of ethylene glycol to the clay on the ceramic tile.

Chemical compositions were obtained using X-ray fluorescence. Ball-milled samples were mixed with the lithium metaborate in a 1:10 ratio, fired at 900 °C, and molded into a 20-mm-wide disc. Oxide abundances were determined by a ZAF algorithm. Total H_20 and CO_2 contents were measured using a CHN analyzer.

Visible to near-infrared (350–2600 mm) diffuse-reflectance spectra were obtained using a Beckman UV5240 spectrophotometer with a Halon-coated integrating sphere. The spectra were first converted to a Kubulka-Munk remission function, which is defined as $F(R) = (1 - R)^2/2R \approx k/s$, where R is reflectance, k is absorption coefficient, and s is the scattering coefficient. To the extent that the scattering coefficient is independent of wavelength, the Kubulka-Munk remission function will approximate the absorption spectrum. Each converted spectrum was fit to a sum of Gaussian bands on a constant baseline. The fitting parameters were entirely unconstrained.

Mineralogical and chemical results

The two Smithsonian samples consist predominantly of dioctahedral smectite based on (060) d spacings of 1.49–1.50 Å (Table 1). NMNH R7452 contains pollucite (a Cs-rich zeolite); NMNH 101836 contains only quartz as an accessory phase. Sample K-P (Foord et al., 1986) contains about 20% admixed cookeite.

0003–004X/88/0102–0140$02.00

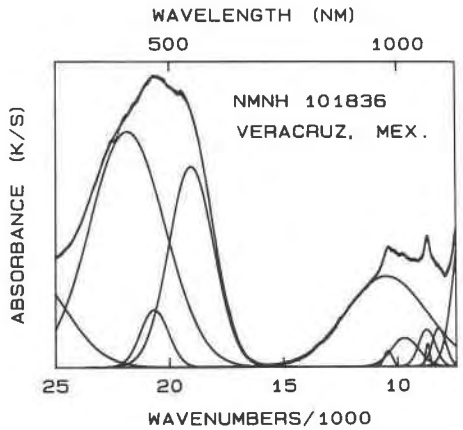

Fig. 1. Diffuse-reflectance spectra and model deconvolution of NMNH 101836. Bands at 10 400, 18 800, 20 600, and 22 400 cm^{-1} result from electronic transitions of Mn^{3+}. The weak, sharp bands near 9000 cm^{-1} are overtone and combination bands of interlayer H_2O and structural OH.

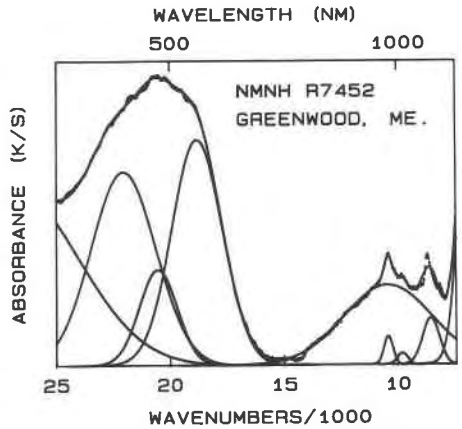

Fig. 2. Diffuse-reflectance spectra of NMNH R7452. Bands in the spectra are as in Fig. 1.

All of the samples have an interlayer thickness of about two water layers ($d_{001} \approx 15$ Å) and expand along c^* to about 17 Å when glycol saturated. Upon K saturation, the (001) spacing collapses to 12.8 Å (NMNH R7452) and 13.8 Å (NMNH 101836) indicating a low negative charge on the silicate lattice characteristic of smectite rather than vermiculite. Heat treatment produces further collapse to 10.16 and 9.93 Å. A normal smectite heated to 550 °C for 2 h should collapse to a d_{001} of 10 Å or less (Brindley, 1980). A d_{001} spacing of 10.16 Å in NMNH 101836 suggests the presence of minor interlayer hydroxycation.

Structural formulae cast from chemical analyses (Table 2) indicate that the three samples are nearly pure montmorillonite. The layer charges range from −0.57 to −1.32 consistent with the K-saturation results. Note that, in the structural formula representations, the number of octahedral cations are forced to total no more than 2.00 with any extra Mg assigned to the interlayer.

Results and discussion

Diffuse-reflectance spectra of the montmorillonite samples NMNH 101836, NMNH R7452, and K-P are shown in Figures 1, 2, and 3, respectively. From the fitting procedure (Table 3), absorption bands are found near 10 400, 18 800, and 20 600, and 22 400 cm^{-1}. Several sharp absorption features interfere with the broad band centered near 10 400 cm^{-1}. These features are due to overtone and combination vibrational modes of interlayer H_2O and structural OH.

The energies, widths, and relative intensities of the bands found in the montmorillonite spectra are characteristic of Mn^{3+} but not Mn^{2+}. A similar set of absorption bands is found in manganian (Mn^{3+} andalusite (Hålenius, 1978) and in piemontite (Burns, 1970). In contrast, the three lowest-energy absorption bands observed in the spectra of Mn^{2+} silicates are found near 19 400 cm^{-1} (515 nm), 23 000 cm^{-1} (435 nm), and 24 500 cm^{-1} (408 nm) (e.g., Keester and White, 1968). Those bands are due to the $^6A_1 \rightarrow {}^4T_1$, $^6A_1 \rightarrow {}^4T_2$, and $^6A_1 \rightarrow {}^4E,{}^4A_1$ ligand-field transitions of octahedrally coordinated Mn^{2+}. No evidence of such Mn^{2+} bands are present in the montmorillonite spectra. It should be pointed out, however, that the small Mn content (ca. 0.1%) would not show any absorption bands if the Mn is in the 2+ oxidation state inasmuch as the Mn^{2+} ligand-field transitions are spin-forbidden and have very low absorption coefficients.

The effect of Fe^{3+} on the spectra should also be men-

Table 1. Observed d spacings in montmorillonite samples

Sample	060	001 AD	001 G	001 K	001 HT
NMNH 101836	1.490	15.2	17	13.8	10.16
NMNH R7452	1.490	15.0	17	12.8	9.93

Note: AD = air dried; G = glycol saturated; K = K saturated; HT = heat treated at 550 °C for 2 h.

Table 2. Chemical compositions and structural formulas

Sample:	101836	R7452	K-P*
SiO_2	55.68	48.24	56.3
Al_2O_3	20.94	22.39	20.0
Fe_2O_3	0.42	0.50	1.32
MnO	0.15	0.16	1.38
MgO	2.59	3.76	2.63
CaO	2.51	2.26	0.75
Na_2O	0.33	<0.1	0.69
K_2O	0.05	0.25	0.52
H_2O (tot.)	19.5	22.4	16.4
Total	102.2	100.3	100.0

Structural formulas

NMNH 101836: $(Ca_{0.38}Na_{0.09}K_{0.01})(Al_{3.38}Mg_{0.55}Mn_{0.018})(Si_{7.88}Al_{0.12})O_{20}(OH)_4$

NMNH R7452: $(Ca_{0.43}Mg_{0.2})(Al_{3.33}Mg_{0.65}Mn_{0.02})(Si_{7.33}Al_{0.67})O_{20}(OH)_4 \cdot xH_2O$

K-P: $(Ca_{0.12}Mg_{0.05}Na_{0.18}K_{0.1})(Al_{3.28}Fe_{0.14}Mg_{0.51}Mn_{0.07})(Si_{7.9}Al_{0.08})O_{20}(OH)_4 \cdot xH_2O$

* Data for sample K-P, normalized to 100%, are taken from Foord et al. (1986).

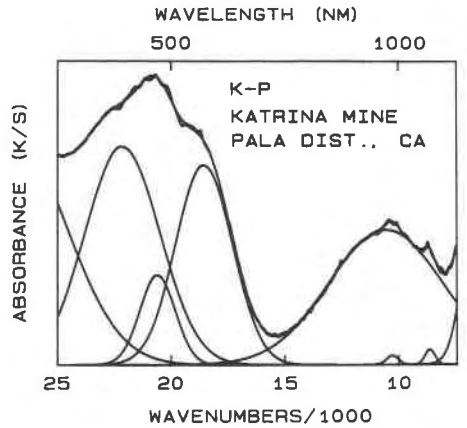

Fig. 3. Diffuse-reflectance spectra of sample K-P (Foord et al., 1986). Bands in the spectra are as in Fig. 1.

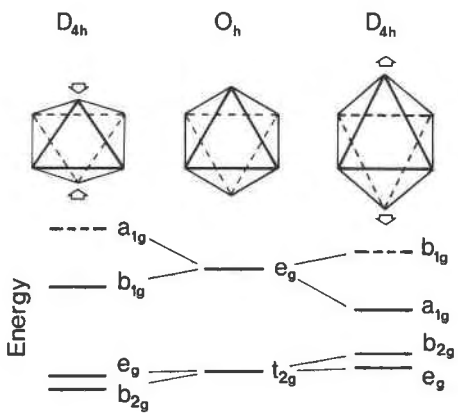

Fig. 4. Mn^{3+} $3d$ energy levels in (a) tetragonal distortion with z ligands in, (b) regular octahedron, and (c) tetragonal distortion with z ligands out. Orbitals that are unoccupied are indicated by dashed lines. The ligand-field theory parameter $10Dq$ (the $t_{2g} - e_g$ orbital separation in O_h symmetry) is given by the $b_{1g} - b_{2g}$ orbital energy separation in D_{4h} symmetry.

tioned. The energies of Fe^{3+} bands in montmorillonite should be similar to those in nontronite. Octahedrally coordinated Fe^{3+} in nontronite shows bands at 10 600 cm^{-1} (943 nm), 16 100 cm^{-1} (621 nm), 22 500 cm^{-1} (444 nm) corresponding to the $^6A_1 \rightarrow {}^4T_1$, $^6A_1 \rightarrow {}^4T_2$, and $^6A_1 \rightarrow {}^4E$, $^4A_1$ ligand-field transitions (Sherman and Vergo, in prep.; see also, Karickhoff and Bailey, 1973; Singer, 1982). Note that the Fe^{3+} ligand-field transitions, like those of Mn^{2+}, are nominally spin-forbidden. Bands due to small amounts of Fe^{3+} would be obscured by the more intense Mn^{3+} bands. Attempts to include bands due to Fe^{3+} ligand-field transitions in the fitting procedure were unsuccessful.

The Mn^{3+} cation has four $3d$ electrons; in an octahedral field, the ground state $3d$ orbital electronic configuration would be $t_{2g}^3 e_g^1$. Only a single spin-allowed electronic transition would be possible, $^5E_g \rightarrow {}^5T_{2g}$, corresponding to the $t_{2g} \rightarrow e_g$ one-electron orbital transition. This should occur near 20 000 cm^{-1} (500 nm) based on SCF-Xα-SW molecular orbital calculations (Sherman, 1984) and the spectra of other Mn^{3+} minerals. As is well-known, however, the Mn^{3+} cation distorts its coordination site via the Jahn-Teller effect. The distortion decreases the symmetry of the coordination site from octahedral (O_h) to tetragonal (D_{4h}). Under the tetragonal distortion, the $t_{2g}(O_h)$ orbital splits into $e_g(D_{4h})$ and $b_{2g}(D_{4h})$ orbitals, whereas the $e_g(O_h)$ orbital is split into $a_{1g}(D_{4h})$ and $b_{1g}(D_{4h})$ orbitals (Fig. 4). Hence, in a tetragonal site, three absorption bands will be observed instead of one. The presence of four bands in the montmorillonite spectra results from further distortion of the tetragonal site to one with orthorhombic (C_{2v}) or smaller symmetry. This further distortion splits the $e_g(D_{4h})$ orbital into singly degenerate $a_1(C_{2v})$ and $b_1(C_{2v})$ orbitals.

From the band energies, it is possible to get an approximate estimate of the Mn–O bond lengths and the degree of distortion of the Mn^{3+} coordination site. To do this, however, we must assign the bands to the specific electronic transitions. For a first approximation, we shall assume that the octahedral Mn^{3+} site has only undergone the tetragonal distortion. Two different possible tetragonal distortions of the MnO_6 coordination site must be considered, however, depending upon whether the axial Mn–O bonds are extended or compressed relative to the equatorial Mn–O bonds. The one-electron energy levels for Mn^{3+} in both tetragonal distortion schemes are shown in Figure 4.

In D_{4h} (tetragonal) symmetry, the Mn $3d$ orbital energies are described in terms of the parameters Ds, Dt, and Dq (Table 4), where Dq is the cubic crystal field splitting and Ds, Dt describe the tetragonal field (Perumareddi, 1967; Konig and Kremer, 1977). If the tetragonal distortion is such that the axial Mn–O bonds are compressed relative to the equatorial bonds (Fig. 4), then the bands

TABLE 3. Energies and assignments of Mn^{3+} ligand-field bands in montmorillonite spectra

Assignment*		NMNH 101836	NMNH R7452	K-P
D_{4h}	C_{2v}			
$^5B_{1g} \rightarrow {}^5A_{1g}$	$^5B_1 \rightarrow {}^5A_1$	10 480	10 276	10 542
$^5B_{1g} \rightarrow {}^5B_{2g}$	$^5B_1 \rightarrow {}^5A_1$	19 041	18 751	18 560
	$^5B_1 \rightarrow {}^5B_2$	20 660	20 496	20 605
$^5B_{1g} \rightarrow {}^5E_g$	$^5B_1 \rightarrow {}^5A_2$	21 837	22 127	22 143

* The notation given is for the actual (multielectronic) spectroscopic states: the $B_{1g} \rightarrow A_{1g}$, $B_{1g} \rightarrow B_{2g}$ and $B_{1g} \rightarrow E_g$ spectroscopic transitions correspond to the $a_{1g} \rightarrow b_{1g}$, $b_{2g} \rightarrow b_{1g}$, and $e_g \rightarrow b_{1g}$ one-electron-orbital transitions of Mn^{3+} in a tetragonal site.

TABLE 4. Orbital energies in the tetragonal crystal field

Orbital	Energy
b_{1g}	$2Ds - Dt + 6Dq$
a_{1g}	$-2Ds - 6Dt + 6Dq$
b_{2g}	$2Ds - Dt - 4Dq$
e_g	$-Ds + 4Dt - 4Dq$

at 10400 and 22400 cm^{-1} correspond to the $b_{1g} \rightarrow a_{1g}$ and $b_{2g} \rightarrow a_{1g}$ transitions, and the two bands at 18800 and 20600 cm^{-1} correspond to the split $e_g \rightarrow a_{1g}$ transition. Using the orbital energy expression in Table 4, it follows that $10Dq$, Ds, and Dt are 12000, -1871, and -583 cm^{-1}. The value for $10Dq$ in this energy-level scheme, however, is unrealistically small for a trivalent cation octahedrally coordinated by oxygen.

If, instead, it is assumed that the axial Mn–O bonds are extended relative to the equatorial Mn–O bonds (Fig. 4c), the bands at 10400 and 18800 cm^{-1} would be assigned to the $a_{1g} \rightarrow b_{1g}$ and $b_{2g} \rightarrow b_{1g}$ transitions, whereas the bands at 20600 and 22400 cm^{-1} would be split components of the $e_g \rightarrow b_{1g}$ transition. This energy-level scheme implies that $10Dq$, Ds, and Dt are 18800, 1934, and 533 cm^{-1}. The more reasonable value for $10Dq$ suggests that this energy-level scheme is correct.

The value for $10Dq$ for Mn^{3+} in Al_2O_3 is 19470 cm^{-1} (McClure, 1962), whereas $10Dq$ for the Mn^{3+} aquo-complex is 21000 cm^{-1} (Orgel, 1966). Hence, the value estimated for Mn^{3+} in montmorillonite (18800 cm^{-1}) is quite reasonable. It should be pointed out, however, that nearly all of the previous calculations in the mineral literature of "$10Dq$" for Mn^{3+} cations occupying distorted sites in minerals have been done incorrectly. A common mistake is to assume that $10Dq$ corresponds to the average energy of the $e_g(O_h)$-derived states minus the average energy of the $t_{2g}(O_h)$-derived states. In the case of a tetragonally distorted site, for example, this quantity calculated from the spectra would not correspond to $10Dq$ but instead would be $10Dq - 5Dt - Ds/2$. For this reason, "$10Dq$" for Mn^{3+} cations are often quoted in the mineral literature as being between 10000 and 15000 cm^{-1} instead of more realistic values between 18000 and 22000 cm^{-1}.

As noted previously, the presence of four bands shows that the symmetry of the Mn^{3+} coordination site is not D_{4h} but must be C_{2v} or lower. The assignments of the bands in terms of C_{2v} symmetry is given in Table 3. The C_{2v} symmetry, all the transitions are Laporte-allowed except the $^5B_1 \rightarrow {}^5B_2$. The band at 20600 cm^{-1}, therefore, must correspond to that transition since it is much weaker than the other Mn^{3+} ligand-field bands.

We can now use the values of $10Dq$ and Dt to estimate the degree of tetragonal distortion in the Mn^{3+} site. The tetragonal field parameter Dt is a measure of the difference between the Dq parameters associated with the z-axis ligands and the xy-axes or equatorial ligands (e.g., Douglas and Hollingsworth, 1985):

$$Dt = -\tfrac{4}{7}[Dq(z) - Dq(xy)] = 533 \text{ cm}^{-1}.$$

If we assume that the derived Dq parameter is an average of that for the two oxygen types, then

$$Dq = \tfrac{1}{6}[2Dq(z) + 4Dq(xy)] = 1880 \text{ cm}^{-1}.$$

Solving the two equations, we get $Dq(xy) = 2191$ cm^{-1} and $Dq(z) = 1258$ cm^{-1}. The significant difference between $Dq(xy)$ and $Dq(z)$ implies that the tetragonal distortion of the site is quite large. Using the approximation of ligand-field theory, we have $Dq \propto (1/r)^5$ where r is the M–O bond length. Hence,

$$r(xy)/r(z) = [Dq(z)/Dq(xy)]^{1/6} = 0.895.$$

The average Mn–O bond length should be about 2.04 Å given the ionic radius of Mn^{3+} and the observed value for $10Dq$. It follows that $r(xy) \approx 1.96$ and $r(z) \approx 2.19$.

The ionic radius of Mn^{3+} is nearly identical to that of Fe^{3+}. One might expect that a manganian (Mn^{3+}) smectite (analogous to nontronite) might be stable or, at the very least, that extensive solid solution between such a hypothetical end member and nontronite could occur. The absence of such Mn^{3+} smectites may simply reflect the limited stability of Mn^{3+} in most geochemical environments. In addition, however, the large tetragonal distortion of the Mn^{3+} coordination site may limit the extent of the solid solution of Mn^{3+} in montmorillonite inasmuch as the z-axis elongation should strain the octahedral Al(O,OH) sheet.

Acknowledgments

Thanks are due to P. Dunn (National Museum of Natural History) for providing access to samples 101836 and R7452 in the collection of the National Museum. E. Foord (U.S. Geological Survey) provided sample K-P and associated data for this material along with helpful discussions. XRF analyses were done by B. Scott (USGS) and total H_2O determinations were provided by Z. A. Brown (USGS). S. Altaner, C. Lawson, M. Ross, and K. Langer provided helpful comments.

References cited

Brindley, G.W. (1980) Order-disorder in clay mineral structures. In G.W. Brindley and G. Brown, Eds., Crystal structures of clay minerals and their X-ray identification, p. 125–126. Mineralogical Society, London.

Burns, R.G. (1970) Mineralogical applications of crystal field theory. Cambridge University Press, Cambridge.

Douglas, B.F., and Hollingsworth, C.A. (1985) Symmetry in bonding and spectra, an introduction. Academic Press, Orlando, Florida.

Foord, E.E., Starkey, H.C., and Taggart, J.E. (1986) Mineralogy and paragenesis of "pocket" clays and associated minerals in complex granitic pegmatites, San Diego County, California. American Mineralogist, 71, 428–439.

Hålenius, U. (1978) A spectroscopic investigation of manganian andalusite. Canadian Mineralogist, 16, 567–575.

Jackson, M.L. (1956) Soil chemical analysis—Advanced course. Published by the author, Department of Soil Science, University of Wisconsin, Madison, Wisconsin.

Karickhoff, S.W., and Bailey, G.W. (1973) Optical absorption spectra of clay minerals. Clays and Clay Minerals, 21, 59–70.

Keester, A.S., and White, W.B. (1968) Crystal field spectra and chemical bonding in manganese minerals. In Papers and Proceedings of the Fifth General Meeting, International Mineralogical Association, 1966, p. 22–35. Mineralogical Society, London.

Kinter, E.B., and Diamond, S. (1956) A new method for preparation and treatment of oriented aggregate samples of soil clays for X-ray diffraction analysis. Soil Science, 81, 111–120.

Konig, E., and Kremer, S. (1977) Ligand field energy diagrams. Plenum Press, New York.

McClure, D.S. (1962) Optical spectra of transition metal ions in corundum. Journal of Chemical Physics, 36, 2757–2779.

Orgel, L.E. (1966) An introduction to transition metal chemistry: Ligand field theory. Methuen, London.

Perumareddi, J.R. (1967) Ligand field theory of d^3 and d^7 electronic configurations in noncubic fields: I. Wave functions and energy matrices. Journal of Physical Chemistry, 71, 3144–3154.

Ross, C.S., and Hendricks, S.B. (1945) Minerals of the montmorillonite group and their origin and relations to soils and clays. U.S. Geological Survey Professional Paper 205-B, 79 p.

Sherman, D.M. (1984) Electronic structures of manganese oxide minerals. American Mineralogist, 67, 788–799.

Singer, R.B. (1982) Spectral evidence for the mineralogy of the high albedo dusts and soils on Mars. Journal of Geophysical Research, 87, 10159–10168.

Weaver, C.E., and Pollard, L.D. (1973) The chemistry of clay minerals. Developments in Sedimentology, 15, 213 p.

Manuscript received October 22, 1986
Manuscript accepted September 23, 1987